

HETEROCYCLES, Vol. 79, 2009, pp. 471 - 486. © The Japan Institute of Heterocyclic Chemistry  
Received, 16th July, 2008, Accepted, 5th August, 2008, Published online, 11th August, 2008.  
DOI: 10.3987/COM-08-S(D)4

**SUBTLE CONTROL IN SOLUTION AND CRYSTAL STRUCTURES  
WITH WEAK HYDROGEN BONDS: THE UNUSUAL PROFILE OF  
DIMETHYL 3, 12-DIOXO-7, 8 DITHIA 4,  
11-DIAZABICYCLO[12.2.2]OCTADEC-1(16), 14, 17-TRIENE 5,  
10-DICARBOXYLATE (TDA1)**

**Isabella L. Karle,<sup>a\*</sup> Lulu Huang,<sup>a</sup> Punna Venkateshwarlu,<sup>b</sup> A. V. S. Sarma,<sup>c</sup>  
and Subramania Ranganathan<sup>b\*</sup>**

<sup>a</sup>Laboratory for the Structure of Matter, Naval Research Laboratory, Washington,  
D.C. 20375-5341

<sup>b</sup>Discovery Laboratory, Organic III, Indian Institute of Chemical Technology,  
Hyderabad 500 607, India

<sup>c</sup>Centre for NMR, Indian Institute of Chemical Technology, Hyderabad 500 607,  
India

E-mail: isabella.karle@nrl.navy.mil; ranga@iict.res.in

In memory of John W. Daly, an ultimate naturalist and inspiring scientist whose studies of the beautiful, highly toxic, South American tropical frogs and their ecology, biology, chemistry and pharmaco-dynamics opened new avenues for intellectual pursuits. His memory and legacy will reside with those who had the pleasure of sharing his investigations.

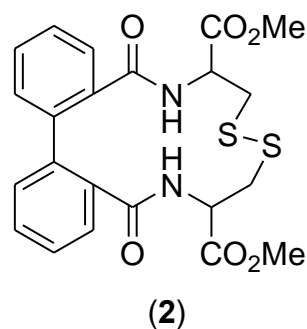
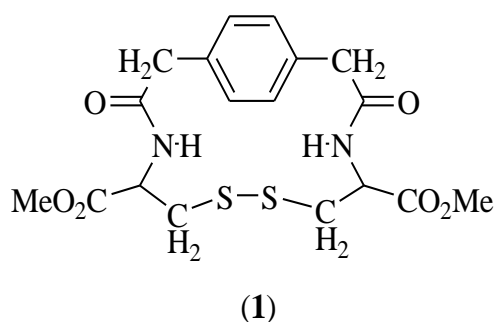
**Abstract** – The structural features of the title compound were determined or examined by three diverse procedures: single crystal X-ray diffraction analysis, solution spectroscopic procedures and quantum mechanical theoretical calculations. The conformational asymmetry of the macrocycle provides the opportunity to form one strong N-H···O-C intermolecular hydrogen bond, as well as, a number of weak C-H···O-C bonds. The interior of the macrocycle has short approaches for N-H··· $\pi$  and N-H···S. The many weak hydrogen bonds cooperate to form a very hard, robust crystal. Crystal parameters: C<sub>18</sub>H<sub>22</sub>N<sub>2</sub>O<sub>6</sub>S<sub>2</sub>, P2<sub>1</sub>2<sub>1</sub>2<sub>1</sub>, a = 5.108(1) Å, b = 18.948(4) Å, c = 21.029(3) Å,  $\alpha = \beta = \gamma = 90^\circ$ . Quantum chemical calculations have provided a strong foundation for

weak hydrogen bonds. Contrary to popular belief, the present work has conclusively proved that the importance of weak hydrogen bonds is perhaps underestimated.

## INTRODUCTION

The surprising finding that the hard, dense crystalline material **2** formed by condensation of diphenic anhydride and Cystine-di-OMe, on crystallographic examination provided a structure that was free of water and normal hydrogen bonds.<sup>1</sup> An incisive analysis with support from the literature, suggested that the rigidity in the crystal arises from traditionally weak hydrogen bonds and  $\text{CH}\cdots\pi$  bonding with the aromatic system, along each of the three axes of the crystal.<sup>2</sup> The importance of weak hydrogen bonds is currently receiving significant attention, because of the role that they can play in shaping structures. Their advantages are in numbers and cooperativity.

We felt that a more detailed exploration of this area, along with support for such structures in terms of energies by quantum calculations, would place the domain in a stronger foundation. An excellent example for the study of these phenomena, along with others, presented itself from **1**, formed readily from 1,4-phenylene diacetic chloride with Cystine-di-OMe in 10% yield.



Prior to the results from the X-ray, the compound was assigned as the 1:1 adduct **1** structure rather than the otherwise expected 2:2 adduct (paracyclophane) **3** on the basis of an interesting application of mass spectrometry. The original mass spectrum of **1** had a base peak  $(\text{M}+\text{H})^+$  (427) and an  $(\text{M}_2+\text{H})^+$  peak at 853 (30%). The presence of the peak at 427 strongly suggested a monomeric structure for the compound that could form transient complexes with  $\text{H}^+$  in the mass spectrometer. To establish the nature of the compound the MS-MS experiment was performed on the peak at 853  $(\text{M}_2+\text{H})^+$ . In the event that they represent the monomeric complexes, their irradiation should show clean reversal to the monomeric peak at 427. MS-MS on the 853  $(\text{M}_2+\text{H})^+$  peak clearly formed the monomer peak at 427 (Figure 1) suggesting the monomeric structure **1** for the compound.<sup>3</sup> This was confirmed by X-ray crystallography. Compound **1** gave colorless needles from MeOH, mp 215-220 °C, one of which was used for X-ray crystallography.

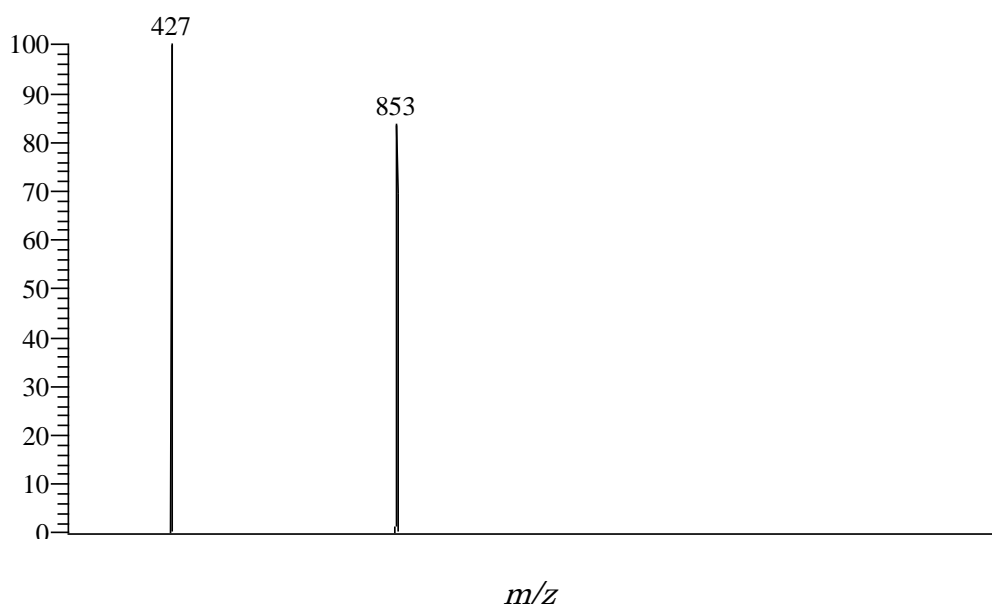


**Figure 1.** MS MS of **1**

## RESULTS

### Crystal Structure

An ORTEP diagram of **1** is shown in Figure 2. The plane of the aromatic ring is nearly orthogonal to the mean plane of the macrocycle. The molecule has only very approximate 2-fold rotational symmetry, since the need for maintaining an orthogonal value for the C-S-S-C dihedral angle<sup>4</sup> in a relatively small macrocycle causes large deviations from any rotational symmetry. The two amide moieties, -C(O)-NH-, have atoms that are nearly coplanar with the usual trans conformation. For steric reasons, the ester groups are extended away from the central ring. Relevant torsional angles are listed in Table 1. The crystallographic data are listed in Table 2.

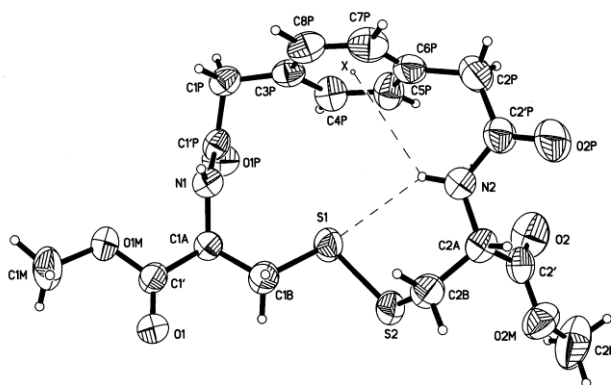


**Figure 2.** ORTEP drawing of TDA1 with anisotropic thermal parameters. The dashed lines represent internal hydrogen bonds.

**Table 1.** Torsional angles (deg.) in macrocycle

left side		right side	
C2B S2 S1 C1B	-88.7		
S2 S1 C1B C1A	-164.3	-87.2	S1 S2 C2B C2A
S1 C1B C1A N1	-59.3	+76.5	S2 C2B C2A N2
C1B C1A N1 C1'P	+109.6	+162.0	C2B C2A N2 C2'P
C1A N1 C1'P C1P	-170.1	+173.0	C2A N2 C2'P C2P
N1 C1'P C1P C3P	+80.7	+12.4	N2 C2'P C2P C6P

**Table 2.** Crystal data and structure refinement for TDA1

Identification	CCDC# 692686	Theta range for data	3.1° to 65.0°
Empirical formula	C <sub>18</sub> H <sub>22</sub> N <sub>2</sub> O <sub>6</sub> S <sub>2</sub>	Index ranges	-1 < h < 17
Formula weight	426.5		-1 < k < 22
Temperature, K	293(2)		-1 > l > 24
Wavelength, Å	1.54178	Reflections collected	2649
Space group	P2 <sub>1</sub> 2 <sub>1</sub> 2 <sub>1</sub>	Independ. refl	2445
[R(int)=0.0484]			
Unit cell dimensions		No. refl. observed >2σ(I)	2123
a = 5.1080(10) Å		Absorption correction	Semi-empirical
b = 18.948(4) Å		Refinement method	Full-matrix least-squares on F <sup>2</sup>
c = 21.029(3) Å			
α = 90°, β = 90°, γ = 90°			
Volume	2035.3(7) Å <sup>3</sup>	Data/restraints/parameters	2445/0/255
Z	4	Goodness to fit	1.037
Density (calc.)	1.392 Mg/m <sup>-3</sup>	Final R indices [I > 2(I)]	R1=0.0563
Absorption coefficient	2.701 mm <sup>-1</sup>		wR2=0.1483
F(000)	896	R indices (all data)	R1=0.0646
Color	colorless		wR2= 0.1584
Size	0.70x0.13x0.06mm <sup>3</sup>	Extinc. Coeff.	0.00327
		Flack parameter	-0.0107 (0.0374)

Significant points of interest are the hydrogen bonds that provide links between molecules and maintain the structural framework of the crystal. In the absence of cocrystallized solvent molecules, such as H<sub>2</sub>O, only the two N-H groups are available for classic hydrogen bonding. In fact, the only hydrogen bond with “normal” dimensions is N1-H···O1P that connects molecules in the stacked columns (Table 3). An examination of the stacked molecules in Figure 3 (left), shows three additional near-approaches that flank the stacks, namely CH bonds directed at carbonyl O atoms, C1A-H···O1A, C2AA-H···O2 and C1BH···O1P. The cooperative effect of the “normal” N-H···O bonds and the three “weak” C-H···O bonds between each pair of molecules enhances the stability of the crystal, particularly the columnar stacks that form along the *a* axial direction, and are recognized as a supramolecular assembly. The columns are assembled into sheets parallel to the *b* axis by C1P-H···O2P weak bonds, see Table 3 and Figure 3 (right). Additional lateral connections between the stacks are provided by the extended ester side chains –OMe···OMe, that is, the repeating weak hydrogen bond C1MH···O1M, see Table 3 and Figure 4, along a 2-fold screw axis where D-A = 3.37 Å and H-A = 2.79 Å, Figure 4.

**Table 3.** “Weak” and normal hydrogen bonds

Donor Acceptor		Symmetry of Acceptor	D···A (Å)	DH···A <sup>a</sup> (Å)	∠D-H-A deg(°)
Intermolecular					
N1-H	O1P	1+x,y,z	2.848	2.14	132
C2A-H	O2	1+x,y,z	3.252	2.39	149
C1A-H	O1	-1+x,y,z	3.84 <sup>b</sup>	2.88	174
C1P-H	O2P	1-x,½+y,¾-z	3.393	2.46	164
C1BH	O1P	-1+x,y,z	3.338	2.68	126
C1M-H	O1M	½+x,¾-y,2-z	3.368	2.79	120
Intramolecular					
N2-H	S1	x,y,z	3.607	2.89	137
N2-H	Ring <sup>c</sup>	x,y,z	3.554	2.96	135

<sup>a</sup>DH fixed at 0.90 Å; <sup>b</sup>Extreme limit; <sup>c</sup>NH···π type attraction

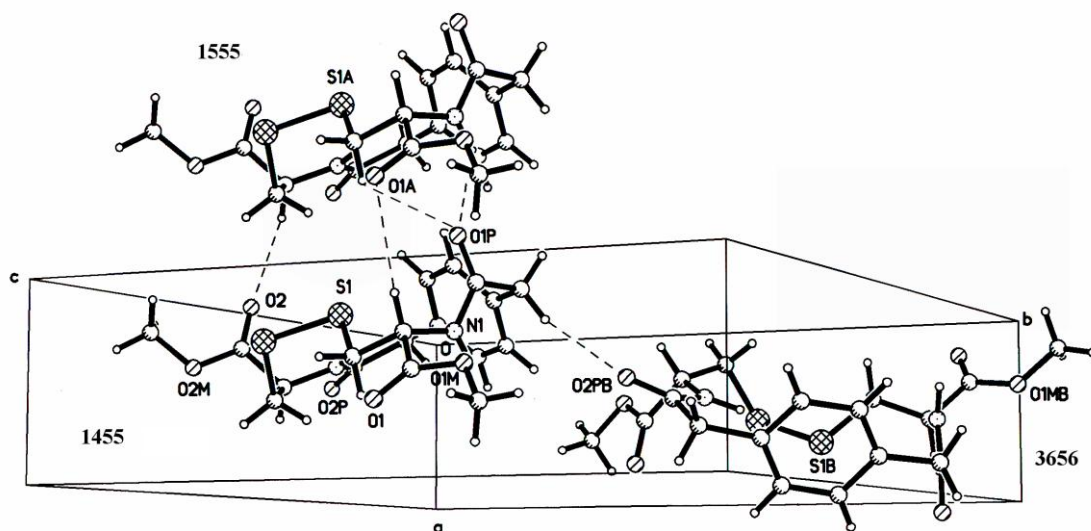


**Figure 3.** Column of TDA1 molecules (left) and sheet (right) connected by weak hydrogen bonds

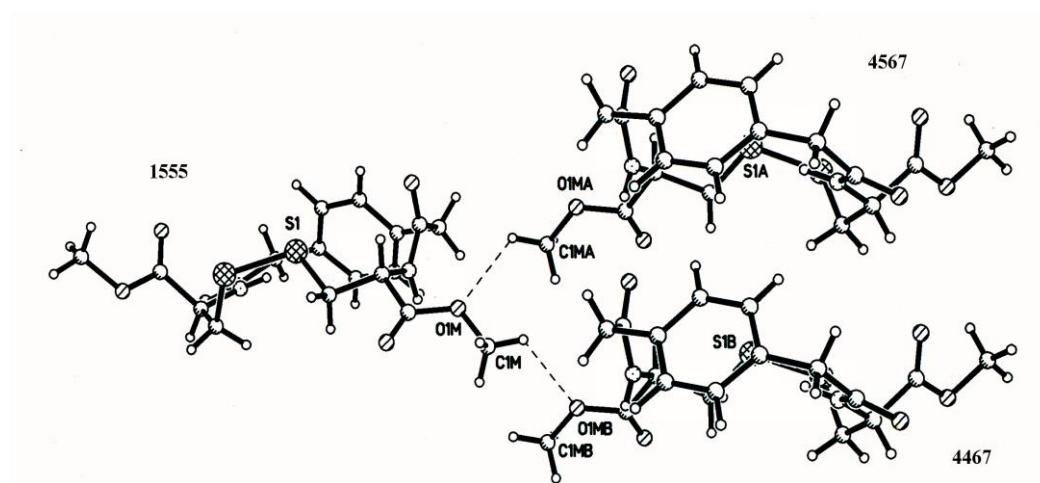


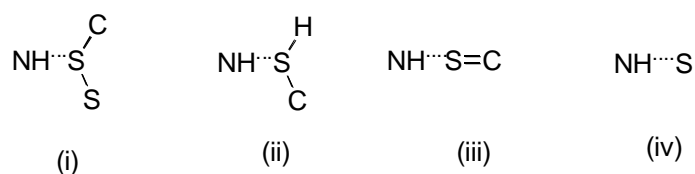
**Figure 4.** Continuous weak  $\cdots\text{OCH}\cdots\text{OCH}\cdots$  bonds between OMe moieties.

This crystal does not exhibit any  $\text{C-H}\cdots\pi$  type bonding. However, in the individual molecules, the  $\text{N2-H}$  bond is directed into the interior of the macrocycle. The H atom is nearly equidistant to S1 and the center of the incorporated phenyl group. There is a contribution to both an  $\text{N2-H}\cdots\text{S1}$  attraction, and also to an  $\text{N2-H}\cdots\pi$  attraction (Table 3 and Figure 2), thus stiffening the macrocycle, as exhibited by the low thermal values for the individual atoms.

In recent years, the importance of “weak hydrogen bonds” has been recognized.<sup>5,6,7,8</sup> In structural chemistry, for example, hydrogen bonding of the type  $\text{C-H}\cdots\text{O}$  instead of  $\text{N-H}\cdots\text{O}$  or hydrogen bonding of the type  $\text{X-H}\cdots\text{Ph}$  (where Ph is a six-membered aromatic ring and the hydrogen bond is directed perpendicularly to the center of the ring) have been observed in crystals in increasing frequency. Desiraju and Steiner<sup>5</sup>

have compiled structures containing weak hydrogen bonds of many types and discussed their geometries and implications. The weak hydrogen bonds have helped in the clarification of intricate differences in molecular properties. The increasing recognition of such weak interactions will set the stage for the better design and understanding of complex structures.

To the author's knowledge there is only one direct comparison in the literature to the  $N2H\cdots S1$  bond (i), which occurs in molecule **2** and has values  $N2\cdots S1 = 3.377 \text{ \AA}$ ,  $N2-H\cdots S1 = 2.78 \text{ \AA}$ , and angle  $N2-H\cdots S1 = 125^\circ$ .<sup>1</sup> Comparable values are listed in the literature for (ii) where  $N\cdots S = 3.43 \text{ \AA}$  and  $H\cdots S = 2.75 \text{ \AA}$  in *N*-acetyl cysteine.<sup>9</sup> Further, Allen *et al.*<sup>10</sup> present data for weak hydrogen bonds in  $N-H\cdots S = C$  (iii), where  $H\cdots S = 2.51 \text{ \AA}$  and  $N\cdots S = 3.43 \text{ \AA}$  and in  $N-H\cdots S$  (iv) where  $H\cdots S = 2.75 \text{ \AA}$  and  $N\cdots S = 3.58 \text{ \AA}$ . If these values can be extrapolated to the present case of (i) (cited above), then the assumption can be made that there is a weak intraring hydrogen bond that contributes to the rigidity of the structure.



Theoretical calculations pertaining to the energy contributions by the weak bonds have been made (*vide infra*).

## SOLUTION STRUCTURE

The ROESY spectrum for **1** presented in Figure 5 not only enabled detailed assignment of peak positions, but also the spatial connectivity. Additionally, it brought out differences in the crystal and solution ( $CDCl_3$ ) structure. The peak assignments derived from the ROESY spectrum are presented in Table 4.

**Table 4.**  $^1H$  NMR for **1** (400 MHz,  $CDCl_3$ ):  $\delta$

$C^\beta H$ ,	2.97,	dd,	2H,	$J=3.7, 14.0 \text{ Hz}$
$C^\beta H'$ ,	3.07,	dd,	2H,	$J=6.4, 14.0 \text{ Hz}$
Bn H,	3.62,	d,	2H,	$J=15.8 \text{ Hz}$
Bn $H'$ ,	3.68,	d,	2H,	$J=15.8 \text{ Hz}$
Ester,	3.73,	s,	6H	
$C^\alpha H$ ,	4.74,	ddd,	2H,	$J=3.7, 6.4, 7.7 \text{ Hz}$
NH,	5.82,	d,	2H,	$J=7.7 \text{ Hz}$
Ar-H,	7.37,	s,	4H	

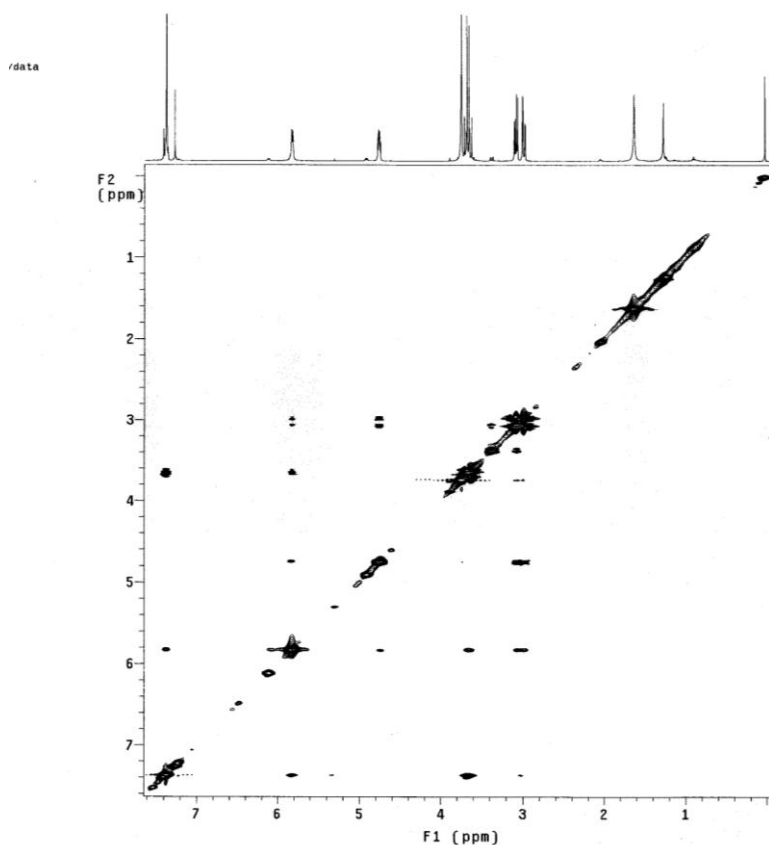


**Figure 5.** The ROESY spectrum of **1**

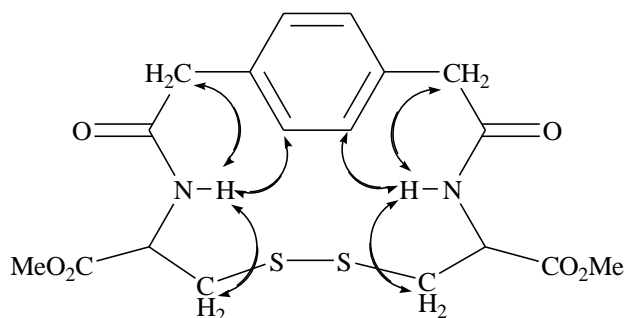


**Figure 6.** Schematic of solution structure

The most striking results from the ROESY spectrum are the exceptional shielding of both the N-H protons by the  $\pi$ -system. To the best of our knowledge, we have not seen an amide N-H appearing at such high fields (5.82 ppm). An interesting observation is that an examination of Figure 2, obtained from X-ray crystallography, clearly shows that while one of the N-H protons is situated where it could be shielded by the  $\pi$ -system, the other N-H proton is orthogonal to it. Thus, subtle energy factors that affect the determination of chemical structures rationalize this fact, as could be seen in Figures 3, in that the N-H proton involved in dimer formation by intermolecular hydrogen bonding is orthogonally placed whereas the other NH is placed in a position more parallel to the plane of the benzene ring, as in Figure 6.



These observations, in conjunction with the fact that in the  $^1\text{H}$ NMR both the hydrogens occur at the highly shielded locations, suggested that in solution both of the N-H protons are turned inwards, as suggested in Figure 6. There must be a gain of additional enthalpic advantage arising from an N-H $\cdots\pi$  interaction. It is possible to twist a ball and stick model of the molecule in the crystal conformation, while preserving the two planar peptides (C1A to C1P and C2A to C2P), the planarity of the dimethylene phenyl (C1P to C2P) and the orthogonal CSSC group, to bring the protons of both N-H groups to be in an appropriate vicinity of the phenyl for N-H $\cdots\pi$  interactions, without any of the other non-bonded pairs of atoms in the molecule coming too close to each other. Finally, the ROESY spectrum also shows spatial connectivity of the N-H with aromatic methylene groups.

The exceptionally strong shielding of the N-H protons by the  $\pi$ -system in solution was strongly supported by the temperature dependent NMR of **1** in  $\text{CDCl}_3$  in the range of 25-45 °C. This afforded a remarkably low  $d\delta/dT$  value of -1.5 ppb/°C, clearly demonstrating strong interaction of the N-H hydrogen with the  $\pi$ -system of the aromatic ring, which is supported by a very low 2.65 Å distance for N-H $\cdots\pi$ .

The chemistry of **1** is rather unique since it has brought in the application of mass spectra, X-ray crystallography and ROESY spectrum to bring out the fine points of structure, that have been augmented by theoretical energy calculations.

## QUANTUM CHEMICAL CALCULATIONS

Quantum chemical calculations on interaction energies in TDA1 were performed using the experimental coordinates taken from its X-ray crystal structure. The 50 atom molecule itself has two intra-molecular weak hydrogen bonds, as shown in Figure 2 (molecule 1555) and also participates in one strong hydrogen bond and several weak hydrogen bonds with surrounding molecules, as shown in Figure 3 (molecules 1555, 1455 and 3656) and in Figure 4 (1555, 4467 and 4567). The geometrical parameters for each of the hydrogen bonds are shown in Table 3.

For obtaining the hydrogen bond energies, we calculated the interaction energy corresponding to hydrogen bond donor and acceptor according to the expression,

$$E_{\text{Hbonding}} \equiv E_{\text{Donor-Acceptor}} - E_{\text{Donor}} - E_{\text{Acceptor}} \quad (1)$$

In order to focus on isolated hydrogen bonds each specific hydrogen bond donor and acceptor group was separated from the rest of their molecular environment in accordance with their representations in Figure 7(a)-(g). It is the interaction energy between each donor and acceptor group indicated in Figure 7(a)-(g) that is used, in accordance with equation (1), to approximate the corresponding hydrogen bond.

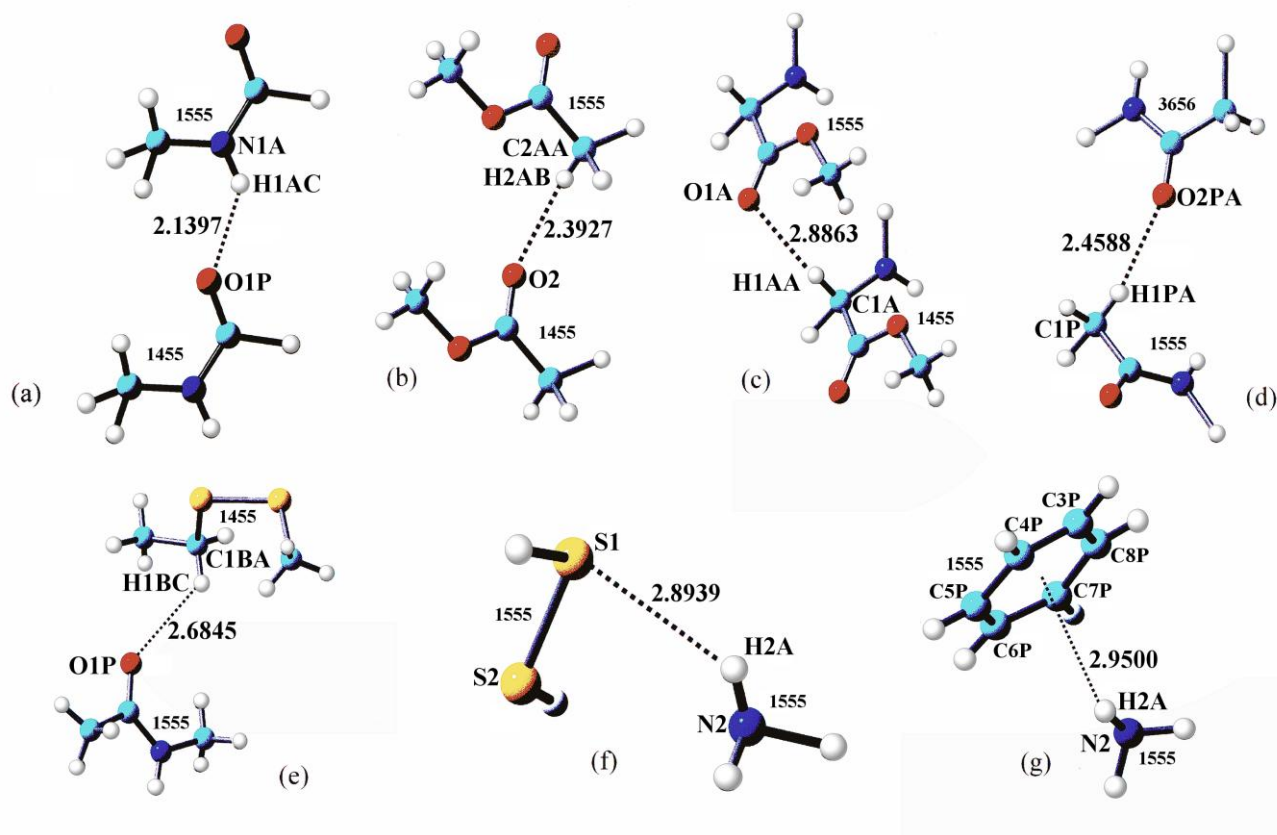


**Figure 7.** Relative positions of atoms, for cases (a)-(g), in the hydrogen bond Donors and Acceptors.

To saturate the bonds that have been severed, in order to separate the hydrogen bond donors and acceptors from the rest of the molecular environment in which they are embedded, hydrogen atoms were placed at the position of the original atom that has been cut away.

Hydrogen bonding between N2-H2A and S1 in Figure 7 (f) is however a special case. Both donor and acceptor in the same molecule are very close to each other. And the geometry is such that if the severed bonds are saturated with hydrogen atoms at the place of the original carbon atoms that have been cut away, the result would be an unrealistic stereo-chemical interaction between them. To avoid imposing an unrealistic perturbation upon the interaction energy representation of the hydrogen bond in question, we used a special automatic feature in the computer program Hyperchem<sup>11</sup> that adds the saturating hydrogen atoms to S2 and N2 that results in a hydrogen to hydrogen distance of 3.2253 Å between them. Figure 7 (g) shows the intra-molecular interaction between an acceptor benzene ring and a hydrogen donor N2-H2A. This interaction is also calculated with equation (1).

We calculated the interaction energies representing each of the hydrogen bonds by the Møller-Plesset perturbation theory.<sup>12,13,14,15,16,17,18</sup> This theory gives significantly more accurate results than those obtained by the

Hartree Fock calculation.<sup>19,20,21,22</sup> The results are listed in Table 5. Successive rows of results are labeled according to the energies  $E_{D+A}$  (the donor-acceptor group as a whole),  $E_D$  and  $E_A$  (the separate Donor and Acceptor, respectively), and  $E_{HB}$  the interaction energy of equation (1), which approximates the hydrogen bond energy (listed in both atomic units and kcal/mol). The trend of calculated hydrogen bond energy magnitudes correlates roughly in an inverse fashion with the length of the hydrogen bond distance. For example the strongest calculated hydrogen bond corresponds to the shortest hydrogen bond distance. Only the  $N-H\cdots\pi$  attraction appears to be very weak.

**Table 5.** Quantum chemical interaction energies associated with hydrogen bonds in TDA1. See explanation in the text.

<b>MP2/6-31G(3df) Calculation:</b>							
[au]	N2-H2A $\cdots S1$	N2-H2A $\cdots \pi$	N1A-H1AC $\cdots O1P$	C2AA-H2AB $\cdots O2$	C1BAH1BC $\cdots O1P$	C1AH1AA $\cdots O1A$	C1PH1PA $\cdots O2PA$
<b><math>E_{D+A}</math></b>	-852.6642	-287.8192	-416.7980	-534.9076	-1611.6412	-645.2224	-416.8738
<b><math>E_D</math></b>	-56.3077	-56.3693	-208.3946	-267.4519	-913.9089	-322.6094	-208.4303
<b><math>E_A</math></b>	-796.3518	-231.4499	-208.3946	-267.4520	-247.7278	-322.6094	-208.4381
<b><math>E_{HB}</math></b>	-0.0047	-0.00002	-0.0088	-0.0037	-0.0045	-0.0036	-0.0054
<b><math>E_{HB}</math></b> [kcal/mol]	-2.935	-0.0127	-5.510	-2.323	-2.814	-2.278	-3.395

**Table 6.** Quantum chemical interaction energies between molecular pairs. See explanation in the text.

<b>MP2/6-31G(3df)</b>	<b>1555-1455</b>	<b>1555-3656</b>	<b>1555-4567</b>
Energy of 2 molecules	-4102.830235 [au]	-4102.800612 [au]	-4102.792121 [au]
Energy of 1 molecule	-2051.394758 [au]	-2051.394758 [au]	-2051.394758 [au]
Interaction Energy between 2 molecules	-0.040719 [au]	-0.011096 [au]	-0.002605
Interaction Energy between 2 molecules	<b>-25.551 [kcal/mol]</b>	<b>-6.963 [kcal/mol]</b>	<b>-1.635 [kcal/mol]</b>

In Table 6 we display the interaction energies between pairs of TDA1 molecules. The entire interaction profile between molecules will in general include more than just the hydrogen bond interactions. Therefore one may notice that the interaction energy between pairs of molecules in Table 6 is not totally accounted for solely in terms of the hydrogen bonds between the donor/acceptor pairs pictured in Figure 7 (a), (b), (c) and (e). For example, the interaction energy of the molecular pair 1555 $\cdots$ 1455 is -25.551 [kcal/mol] when calculated by the MP2 method. The 4 hydrogen bonds between the molecular pair

1555...1455, taken from Table 5 in the MP2 approximation amount to about -13 [kcal/mol], and as expected is considerably less than the total MP2 interaction energy -25.551 [kcal/mol]. Such differences may be accounted for with additional attractive interactions between the molecules of the pair. The weak hydrogen bonds that were considered at the present time all have  $DH\cdots A$  distances less than  $3.0\text{\AA}$ . The differences between the sum of the calculated individual energies and the total energy may be partially accounted for with the numerous additional attractive interactions between  $CH\cdots O$  having  $H\cdots O$  distances greater than  $3.0\text{\AA}$ . Some are shown in Figure 8(a), such as  $C2P-H2PA\cdots O2PA$ . In Figure 8(b), the  $C1MA-H1MF\cdots O1M$  weak bond connects terminal methoxy groups  $OCH_3\cdots OCH_3\cdots OCH_3$  that wind around a 2-fold screw-axes with a  $C-H\cdots O$  distance of  $3.366\text{\AA}$ . Moreover there may be other such interactions between the molecular pairs that have escaped characterization.

All of the energy calculations were implemented using the standard procedures of the computer program Gaussian 03.<sup>23</sup>

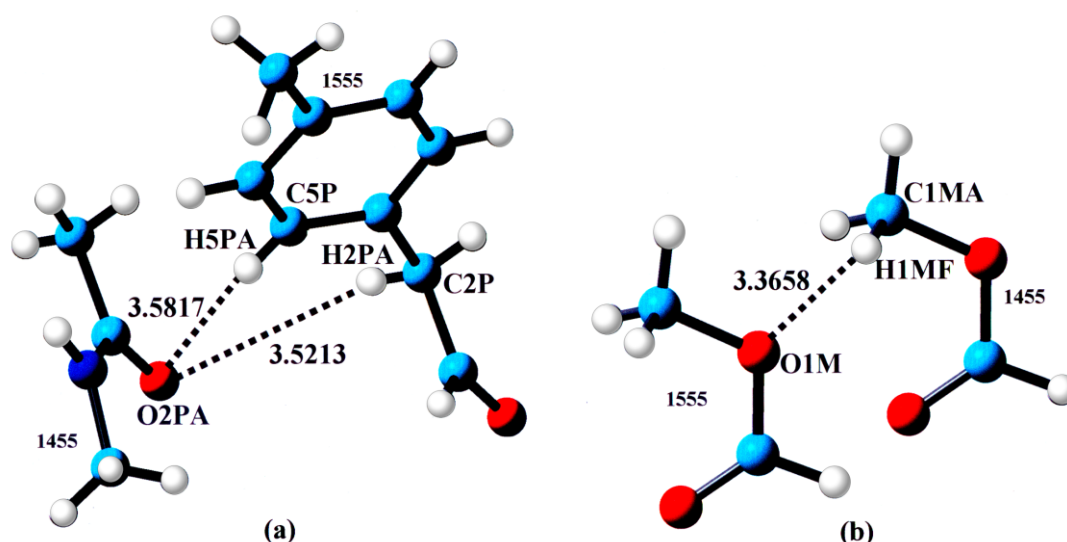


**Figure 8.** Additional weak interactions.

## SUMMARY

Three different procedures have been applied to characterize the TDA1 molecule. They differ in the type of information that they produce and the precision of the information. X-ray diffraction analysis of single crystals deals with the solid state in which a molecule is quite rigid, Figure 2, as are the neighboring molecules, from which intermolecular attractions can be measured in terms of spatial arrangements and precise interatomic distances (e.s.d's  $0.005\text{\AA}$ ). The salient features that were established are one normal  $NH\cdots OC$  intermolecular hydrogen bond, a number of "weak" intermolecular  $CH\cdots OC$  bonds, and two "weak" intramolecular bonds of the type  $NH\cdots S$  and  $NH\cdots \pi$ , all of which contribute to the density, hardness and high melting point of TDA1.

The TDA1 structure of the molecule in solution was obtained from the ROESY spectrum. Obviously the molecule in solution has more freedom of motion and is not constrained by neighboring molecules, thus the results concern an individual molecule. The most striking result is the exceptional shielding of both NH protons by the  $\pi$  system, suggesting that the macrocycle has changed conformation sufficiently for both NH's to be turned inward with respect to the macrocycle and its embedded phenyl ring, rather than just one NH as occurs in the crystal.

The MP2 quantum chemical calculation was based on the coordinates obtained from the X-ray crystal structure. The calculations for the interaction energy contributed by the hydrogen bonds to the total energy show an inverse trend agreeable with the length of the bonds between pairs of atoms except for the magnitude associated with  $\text{NH}\cdots\pi$ . There must be other non-negligible interaction energies between the molecular pair 1555 and 1455, such as shown in Figure 8. In general there is a remarkable agreement between the theoretical calculations and experimental observations.

## EXPERIMENTAL

### General

Melting points were recorded on Fisher-Johns apparatus and are uncorrected. Infrared spectra were recorded on a Thermo Nicolet Nexus 670 spectrometer as KBr pellets and prominent peaks are expressed in  $\text{cm}^{-1}$ .  $^1\text{H}$  and  $^{13}\text{C}$  NMR spectra were recorded on a Varian Gemini 200, Bruker Avance 300, Inova 400 and 500 MHz spectrometers. The chemical shifts are expressed in  $\delta$  (ppm) with TMS at 0.0000 as internal reference. ESI MS was obtained on a micromass QUATTRO-LC instrument and HRMS obtained on a QSTAR XL instrument. Reactions were monitored, wherever possible by TLC. Silica gel G (Merck) was used for TLC and column chromatography was done on silica gel (100-200 mesh). Columns were generally made from slurry in chloroform or hexane and products were eluted with a mixture of chloroform/methanol.

### X-Ray Diffraction

X-Ray data were collected at room temperature with  $\text{CuK}\alpha$  radiation on a Bruker P4 four-circle diffractometer for a total of 2445 independent data and 2123 data observed  $> 2\sigma(I)$ . The structure was solved routinely and refined by full-matrix least squares on  $F^2$  values. The final  $R_1$  value for all of the data was 0.077 and, for the observed data,  $R_1=0.056$  (Table 2). The programs used were those in the SHELXTL package.<sup>24</sup> Tables of coordinates, bond lengths and angles, anisotropic thermal factors, and hydrogen coordinates are deposited with the Cambridge Crystallographic Data Center, CCDC# 692686. Copies of the data can be obtained free of charge on application to the Director, CCDC, 12 Union Road,

Cambridge CB2 1EZ, UK (Fax: +44 1223 336 033; e-mail:deposit@ccdc.cam.ac.uk). Thermal ellipsoids and numbering scheme is shown in Figure 2.

### I. Reaction of 1,4-phenylene diacetic acid chloride with Cystine-di-OMe: Synthesis of 1:1 adduct 1.

To an ice-cooled and well-stirred solution of Cystine-di-OMe.2HCl (1.5 g, 4.4 mmol) in CH<sub>2</sub>Cl<sub>2</sub> (100 mL) was added Et<sub>3</sub>N (0.9 g (1.23 mL), 8.8 mmol) after 0.25 h another lot of Et<sub>3</sub>N (0.9 g (1.23 mL), 8.8 mmol) was added, followed by, after 0.25 h, in drops over period of 0.75 h, a solution of 1,4-phenylene-diacetic acid chloride (0.924 g, 4.0 mmol) in CH<sub>2</sub>Cl<sub>2</sub> (100 mL). The reaction mixture was left stirred at rt overnight, washed with 2N H<sub>2</sub>SO<sub>4</sub> (25 mL), water (20 mL), satd. aq. NaHCO<sub>3</sub> (25 mL), brine (25 mL), dried (Na<sub>2</sub>SO<sub>4</sub>) and evaporated. Crude yield 0.650 g (38%), mp 180-185 °C. Chromatography on silica gel and elution with CH<sub>2</sub>Cl<sub>2</sub>: MeOH (98: 2) afforded 0.174 g (10%), mp 205-210 °C. Crystallization from MeOH afforded colourless needles, mp 215-220 °C. The structure of this compound was established as the 1:1 adduct **1** by spectral data and X-ray crystallography.

<sup>1</sup>H NMR (500 MHz, CDCl<sub>3</sub>): δ 2.97 (dd, *J* = 3.7, 14.0 Hz, 2H, Cyst C<sup>β</sup>Hs), 3.07 (dd, *J* = 6.4, 14.0 Hz, 2H, Cyst C<sup>β</sup>Hs), 3.62 (d, *J* = 15.8 Hz, 2H, Bn Hs), 3.68 (d, *J* = 15.8 Hz, 2H, Bn Hs), 3.73 (s, 6H, CO<sub>2</sub>Me), 4.74 (ddd, *J* = 3.7, 6.4, 7.7 Hz, 2H, Cyst C<sup>α</sup>Hs), 5.82 (d, *J* = 7.7 Hz, 2H, Amide NHs), 7.37 (s, 4H, Ar Hs) (assignment by ROESY)

ESI-MS (*m/z*) (%): 427 (M + H)<sup>+</sup> (100), 853 (M<sub>2</sub> + H)<sup>+</sup> (27), 875 (M<sub>2</sub> + Na)<sup>+</sup> (66) [on MS-MS peak at 853 (M<sub>2</sub> + H)<sup>+</sup> (27) was cleanly fragmented to 427 (M + H)<sup>+</sup> (100) and MS MS peak at 875 (M<sub>2</sub> + Na)<sup>+</sup> (66) was cleanly fragmented to 449 (M + Na)<sup>+</sup> (46)].

### II. Reaction of 1,4-phenylene diacetic acid chloride with Cystine-di-OMe: Synthesis of 1:1 adduct (1) and doubly bridged (1,4) cyclophane 3

To an ice-cooled and well-stirred solution of Cystine-di-OMe.2HCl (1.039 g, 3.047 mmol) in CH<sub>2</sub>Cl<sub>2</sub> (100 mL) was added Et<sub>3</sub>N (1.72 g (2.38 mL), 17.174 mmol) followed by, after 0.5 h, in drops over period of 0.75 h, a solution of 1,4-phenylenediacetic acid chloride (0.639 g, 2.77 mmol) in CH<sub>2</sub>Cl<sub>2</sub> (100 mL). The reaction mixture was left stirred at rt overnight, filtered to yield white powder 0.611 g, mp 165-170 °C, identified as **3** (yield 52%).

IR (KBr): 3289, 1747, 1652, 1540, 1436, 1362, 1217, 1023, 790, 495 cm<sup>-1</sup>

<sup>1</sup>H NMR (500 MHz, DMSO-*d*<sub>6</sub>): δ 2.80-3.30 (m, 8H, Cyst C<sup>β</sup>H<sub>2</sub>s), 3.36-3.51 (m, 8H, Bn Hs), 3.64 (s, 12H, CO<sub>2</sub>Me), 4.40-4.60 (m, 4H, Cyst C<sup>α</sup>Hs), 7.15 (s, 8H, Ar Hs), 8.63 (d, *J* = 7.4 Hz, 4H, Amide NHs)

<sup>13</sup>C (100.580 MHz, DMSO-*d*<sub>6</sub>): δ 38.63 (Cyst C<sup>β</sup>), 41.31 (Bn C), 51.32 (Cyst C<sup>α</sup>), 52.05 (CO<sub>2</sub>Me), 128.72, 133.85 (Ar C), 170.36 (CONH), 170.79 (CO<sub>2</sub>Me)

ESI MS (*m/z*) (%): 875 (M + Na)<sup>+</sup> (100)

HRMS (ESI): *m/z* calculated for C<sub>36</sub>H<sub>44</sub>N<sub>4</sub>O<sub>12</sub>NaS<sub>4</sub> (M+Na)<sup>+</sup> 875.1736, found 875.1750.

The filtrate was washed with 2N H<sub>2</sub>SO<sub>4</sub> (20 mL), water (20 mL), satd. aq. NaHCO<sub>3</sub> (20 mL), water (20 mL), brine (20 mL), dried (Na<sub>2</sub>SO<sub>4</sub>) and evaporated to give 0.412 g of crude product, which was chromatographed on silica gel. Elution with CHCl<sub>3</sub>: MeOH (98: 2) to afforded 0.150 g compound, mp 205-210 °C, identified as **1** (yield 13%).

IR (KBr): 3391, 3334, 1749, 1732, 1654, 1508, 1436, 1320, 1203, 1024, 901, 816, 655, 513 cm<sup>-1</sup>

<sup>1</sup>H NMR (200 MHz, CDCl<sub>3</sub>): δ 2.97 (dd, *J*= 3.9, 14.1 Hz, 2H, Cyst C<sup>β</sup>H<sub>2</sub>s), 3.04 (dd, *J*= 5.5, 14.1 Hz, 2H, Cyst C<sup>β</sup>H<sub>2</sub>s), 3.59 (d, *J*= 15.6 Hz, 2H, Bn Hs), 3.65 (d, *J*= 15.6 Hz, 2H, Bn Hs), 3.74 (s, 6H, CO<sub>2</sub>Me), 4.70-4.79 (m, 2H, Cyst C<sup>α</sup>Hs), 5.80 (d, *J*= 7.81 Hz, 2H, Amide NHs), 7.37 (s, 4H, Ar Hs)

Temperature dependent NMR (400 MHz, CDCl<sub>3</sub>) in the range of 25-45 °C afforded dδ/dT value of -1.5 ppb/°C.

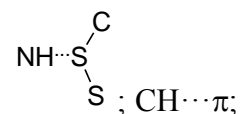
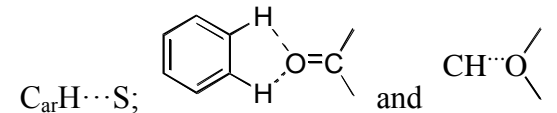
<sup>13</sup>C (75.468 MHz, CDCl<sub>3</sub>): δ 42.18 (Cyst C<sup>β</sup>), 43.52 (Bn C), 52.60 (Cyst C<sup>α</sup>), 52.89 (CO<sub>2</sub>Me), 130.48, 134.58 (Ar C), 170.04 (CONH), 170.89 (CO<sub>2</sub>Me)

HRMS (ESI): *m/z* calculated for C<sub>18</sub>H<sub>22</sub>N<sub>2</sub>O<sub>6</sub>NaS<sub>2</sub> (M+Na)<sup>+</sup> 449.0817, found 449.0810.

## ACKNOWLEDGEMENTS

We thank the Office of Naval Research and the National Institutes of Health Grant GM30902 for supporting the work at the Naval Research Laboratory. P.V. and S.R. are grateful to the Council of Scientific and Industrial Research, New Delhi, for the award of a Fellowship and financial assistance.

## REFERENCES AND NOTES

1. I. L. Karle, P. Venkateshwarlu, and S. Ranganathan, *Biopolymers (Peptide Science)*, 2006, **84**, 502.
2. An analysis shows that the crystal of **2** is supported by the weak hydrogen bonds: ; .
3. In case the peaks at 853 represent complexes of the 2:2 adduct with respectively H<sup>+</sup>, their irradiation would result in a normal fragmentation pattern.
4. I. L. Karle, D. Ranganathan, and V. Haridas, *J. Am. Chem. Soc.*, 1996, **118**, 10916.
5. G. R. Desiraju and T. Steiner, 'The Weak Hydrogen Bond in Structural Chemistry and Biology,' (IUCr Monographs on Crystallography, No. 9) Oxford Science Publications, Oxford, 1999.
6. C. M. Reddy, R. C. Gundakaram, S. Basavoju, M. T. Kirchner, K. A. Padmanabhan, and G. R. Desiraju, *Chem. Commun.*, 2005, 3945.
7. C. D. Tadko and M. L. Waters, *J. Am. Chem. Soc.*, 2004, **126**, 2028.

8. J. C. Lopez, W. Caminati, and J. L. Alonso, [\*Angew. Chem. Int. Ed.\*, 2006, \*\*45\*\*, 290.](#)
9. C. H. Gorbitz and B. Dalhus, *Acta Crystallogr.*, 1996, **C52**, 1756.
10. F. H. Allen, C. M. Bird, R. S. Rowland, and P. R. Raithby, *Acta Crystallogr.*, 1997, **C53**, 680, 696.
11. HyperChem 8.0.3 for Windows, Hypercube, Inc. Gainesville, FL (2007)
12. C. Møller and M. S. Plesset, [\*Phys. Rev.\*, 1934, \*\*46\*\*, 618.](#)
13. M. Head-Gordon, J. A. Pople, and M. J. Frisch, [\*Chem. Phys. Lett.\*, 1988, \*\*153\*\*, 503.](#)
14. M. J. Frisch, M. Head-Gordon, and J. A. Pople, [\*Chem. Phys. Lett.\*, 1990, \*\*166\*\*, 275.](#)
15. M. J. Frisch, M. Head-Gordon, and J. A. Pople, [\*Chem. Phys. Lett.\*, 1990, \*\*166\*\*, 281.](#)
16. M. Head-Gordon and T. Head-Gordon, [\*Chem. Phys. Lett.\*, 1994, \*\*220\*\*, 122.](#)
17. S. Saebø and J. Almløf, [\*Chem. Phys. Lett.\*, 1989, \*\*154\*\*, 83.](#)
18. J. Almlöf, J. K. Faegri, and K. Korsell, [\*L. Comp. Chem.\*, 1982, \*\*3\*\*, 385.](#)
19. C. C. J. Roothaan, [\*Rev. Mol. Phys.\*, 1951, \*\*23\*\*, 69.](#)
20. J. A. Pople and R. K. Nesbet, [\*J. Chem. Phys.\*, 1954, \*\*22\*\*, 571.](#)
21. R. McWeeny and G. Dierksen, [\*J. Chem. Phys.\*, 1968, \*\*49\*\*, 4852.](#)
22. Wikipedia, "Hartree-Fock", <http://en.wikipedia.org/wiki/Hartree-Fock>
23. M. Frisch, *et. al.* Gaussian 03, Gaussian, Inc., Pittsburgh, PA (2003).
24. SHELXTL, Version 5.1, (Bruker AXS, Inc) Madison, WI (USA).